Available online at www.sciencedirect.com
SCIENCE DIRECT
Polymer 46 (2005) 8068–8078
polymer
www.elsevier.com/locate/polymer

Studying the miscibility and thermal behavior of polybenzoxazine/poly(ε-caprolactone) blends using DSC, DMA, and solid state ^{13}C NMR spectroscopy

Jieh-Ming Huang*, Shung-Jim Yang

Department of Chemical Engineering, Vanung University, 1, Van Nung Road, Chung-Li 32054, Taiwan, ROC

Received 22 February 2005; received in revised form 24 June 2005; accepted 28 June 2005
Available online 20 July 2005

Abstract

Polymer blends of polybenzoxazine (PBZ) and poly(ε-caprolactone) (PCL) were prepared by solution blending of PCL and benzoxazine monomer (B-m), followed by thermal curing of B-m. The miscibility and thermal behavior of these PBZ/PCL blends were investigated by differential scanning calorimetry (DSC), dynamic mechanical analysis (DMA), Fourier transform infrared spectroscopy (FTIR), and solid state ^{13}C nuclear magnetic resonance (NMR) spectroscopy. The FTIR spectra indicated that hydrogen bonding interactions occur between the carbonyl groups of PCL and the hydroxyl groups of PBZ upon curing. The DSC results revealed that this PBZ/PCL blend system has a single glass transition temperature over the entire range of compositions that we investigated. The DMA results indicated that the values of T_g of the PBZ/PCL blends were higher than those of the pure polymers. In addition, at higher PCL concentrations we observed two glass transitions for the PBZ/PCL blends: One, for the PCL component, occurred in the low-temperature region and the other, for the PBZ component, in the high-temperature region; this finding indicates that PCL and PBZ are partially miscible in the amorphous phase. The most pronounced effect of the addition of PCL was to broaden the glass transition region, judging from the E'' peaks and the decrease in the value of the loss tangent (tan δ) in the transition region upon increasing the PCL content. We have also studied the ^1H spin-lattice relaxation times in the laboratory frame, T_1^H, and in the rotating frame, $T_{1\rho}^H$, as a function of the blend composition. The T_1^H results are in good agreement with those from the DSC analysis; i.e. the blends are completely homogeneous on the scale of 40–70 nm. The values of $T_{1\rho}^H$ indicate that the PCL present in the blends exists in both crystalline and amorphous phases; the mobility difference between these PCL phases is clearly visible from the $T_{1\rho}^H$ data. In addition, the amorphous phase of PCL is not miscible with PBZ; i.e. it is larger than 2–4 nm.

Keywords: Polybenzoxazine; Poly(ε-caprolactone); Polymer blend

1. Introduction

Polybenzoxazines (PBZs) are a novel class of thermosetting polymers that possess many physical properties that are superior to those of traditional polymers, such as epoxy and phenolic resins. PBZs can be prepared by the Mannich condensation of phenol, formaldehyde, and primary amines [1]. In addition, PBZs can be cured in the absence of a strong acid catalyst and do not produce byproducts during their polymerization. PBZs offer a superb balance of mechanical and physical properties, including low water uptake, near-zero shrinkage, and high thermal stability [2–6], but they tend to be brittle, which is common for phenolic materials, and this feature limits their applications. Therefore, the flexural and impact properties of these resins are expected to improve upon the incorporation of a component having a low glass transition temperature (T_g). Poly(ε-caprolactone) (PCL) is a semi-crystalline polymer that exhibits a very low T_g (−60 °C). PCL is miscible with many polymers, including poly(4-vinyl phenol) (PVPh) [7], poly(benzyl methacrylate) (PBMA) [8], and novolac [9], because the carbonyl groups of PCL can form intermolecular hydrogen bonds with the hydroxyl groups of the second polymer. Because PBZ contains many hydroxyl groups on its main chain after thermal curing, it is anticipated that PBZ may be miscible with PCL as a consequence of intermolecular

* Corresponding author. Tel.: +886 3 4515811 530; fax: +886 3 4514814.
E-mail address: jiehming@msa.vnu.edu.tw (J.-M. Huang).

0032-3861/$ - see front matter © 2005 Elsevier Ltd. All rights reserved.
doi:10.1016/j.polymer.2005.06.104

hydrogen bonding; this situation will contribute to the improved stiffness of the main chain and lead to a range of other favorable properties. Ishida and Lee [10] studied polymer blends of PBZ (B-a type) and PCL and found evidence from FTIR spectra for hydrogen bond formation between the hydroxyl groups of PBZ and the carbonyl groups of PCL. In addition, these blends displayed improved mechanical properties when compared to those of pure PBZ. Recently, Zheng et al. [11] reported that prior to curing, benzoxazine (B-a)/PCL blends are miscible, as evidenced by the behavior of their single and composition-dependant glass transition temperatures and equilibrium melting temperature depressions, but they observed phase separation induced by polymerization after curing at an elevated temperature.

Because the physical properties of polymer blends are influenced strongly by the blending conditions and processes that, in turn, affect the level of mixing of the blends, there is a growing interest in studying the miscibility and phase behavior of polymer blends. Various techniques have been employed to investigate the miscibility of polymer blends, including microscopy, thermal analysis, dynamic mechanical analysis (DMA), dielectric measurements, and spectroscopic measurements [12–15]. Differential scanning calorimetry (DSC) is one of the most widely used techniques for evaluating miscibility—on a scale of 10–30 nm—in terms of the cooperative motion of polymer segments at temperatures close to the glass transition temperature [16,17]. Solid state nuclear magnetic resonance (NMR) spectroscopy is a powerful technique that has been utilized to analyze the miscibility, phase structure, and heterogeneity of polymer mixtures on a molecular scale [18–22]. It is especially useful in polymer blend systems containing complex phase structures that may exist beyond the resolution limits of traditional microscopic or thermal analyses. Two useful proton spin-relaxation times that can be obtained from solid state ^{13}C NMR spectra are the spin-lattice relaxation times in the laboratory frame (T_1^H) and in the rotating frame ($T_{1\rho}^H$). The length scale of heterogeneity—from a few angstroms to some tens of nanometers—can be evaluated approximately from the values of $T_{1\rho}^H$ and T_1^H to allow measurements of compositional heterogeneity on length scales limited by spin diffusion.

A number of investigations have been performed previously to determine the structures of polybenzoxazines using solid state NMR spectroscopy [23–25]. Although there is growing interest in the study of the miscibility and phase behavior of PBZ blends, little attention has been paid so far to the scale of miscibility of PBZ/PCL blends. Therefore, in this study we prepared PBZ/PCL blends by solution blending of PCL and benzoxazine monomer (B-m), followed by thermal curing of B-m. We investigated the thermal properties and dynamic mechanical properties of the blends by DSC and DMA, respectively. In addition, we evaluated the molecular mobility and miscibility of the blends by using solid state ^{13}C NMR spectroscopy.

2. Experimental

2.1. Materials

A sample of PCL having a number-average molecular weight of 10,000 was purchased from Fluka Chemical Co. Bisphenol-A, formaldehyde, and methylamine were purchased from Aldrich Chemical Co. and were used without further purification. Benzoxazine (B-m type) was synthesized from bisphenol-A, formaldehyde, and methylamine according to the procedure presented in Scheme 1 [1]. Aqueous formaldehyde solution (0.4 mol) and dioxane (50 mL) were fed into a three-necked flask under a nitrogen flow and then cooled in an ice bath for 10 min. Methylamine (0.2 mol) dissolved in dioxane (20 mL) was then added slowly into the reactor using a dropping funnel. The mixture was stirred continuously for 20 min before a solution of bisphenol-A (0.1 mol) in dioxane (80 mL) was added. The reaction temperature was raised to 90 °C; the mixture was then heated under reflux for 5 h. The solvent was evaporated under reduced pressure to yield a yellow solid. This crude product was dissolved in ethyl ether and washed three times sequentially with 2 N NaOH and water to remove any impurities and unreacted monomers. The ether solution was dried ($MgSO_4$) and then the solvent was evaporated under reduced pressure. The product was obtained as a pale-yellow viscous fluid.

2.2. Blend preparations

B-m/PCL blends having several different compositions were prepared by solution blending. The polymer mixture was dissolved and stirred in tetrahydrofuran (THF) and then the solution was left to evaporate slowly at 50 °C for 1 day. The samples were then cured sequentially at 120, 140, 160, 180, and 200 °C (for 2 h at each temperature) to ensure total curing of the benzoxazine.

2.3. Infrared spectroscopy

To detect hydrogen bonding in the blends, infrared spectra of polymer blend films were determined using the conventional NaCl disk method. A THF solution containing the blend was cast onto a NaCl disk and dried under conditions similar to those used in the bulk preparation. The film used in this study was thin enough to obey the Beer–Lambert law. FTIR spectra were recorded using a Perkin–Elmer spectra one infrared spectrometer. Each spectrum was obtained at a resolution of 1 cm^{-1}.

2.4. Differential scanning calorimetry

The calorimetric measurements were performed using a differential scanning calorimeter (Perkin–Elmer DSC-7) under a nitrogen atmosphere. The samples (ca. 5 mg), which were placed in a DSC pan, were first heated from 30 to

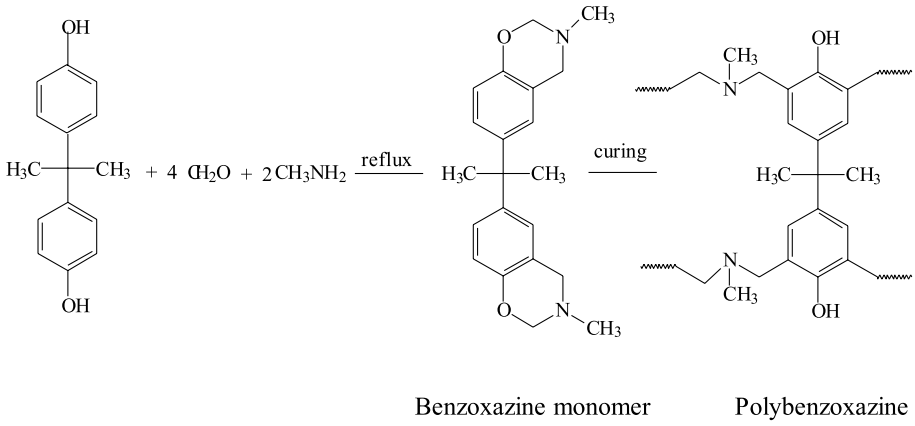

Scheme 1. Preparation of benzoxazine and PBZ.

270 °C at a rate of 10 °C/min (first heating scan) and then maintained at that temperature for 3 min; subsequently, they were cooled to −90 °C at a rate of 10 °C/min. A second scan was then conducted at the same heating rates as those used in the first scan. The midpoint of the change in slope of the plot of the heat capacity of the second heating scan was taken to be the glass transition temperature (T_g). The melting temperature (T_m) was taken as the maximum of the endothermic peak.

2.5. Dynamic mechanical analysis

Dynamic mechanical analysis measurements were performed using a TA Instruments DMA Q800 in a bending mode over a temperature range from −120 to 250 °C. Data acquisition and analysis of the storage modulus (E'), loss modulus (E''), and loss tangent ($\tan\delta$) were recorded automatically by the system. The heating rate and frequency were fixed at 2 °C/min and 1 Hz, respectively. Samples for DMA experiments were prepared using a stainless-steel mold; the sample dimensions were $3\times0.8\times0.2$ cm^3.

2.6. Solid state NMR spectroscopy

High-resolution solid state NMR spectroscopy experiments were performed at ambient temperature (25 °C) using a Bruker AVANCE-400 spectrometer at resonance frequencies of 400.13 and 100.62 MHz for ^{1}H for ^{13}C nuclei, respectively. ^{13}C CP/MAS NMR spectra were recorded using a CP contact time of 1 ms, a repetition time of 4 s, and a spinning speed of 6.2 kHz. The chemical shifts of ^{13}C nuclei were referenced externally to tetramethylsilane (TMS). The proton spin-lattice relaxation times in the laboratory frame (T_1^H) were measured, using the inversion-recovery method, by monitoring the decays of the peak intensities of specific carbon atoms after a π–τ–π/2 inversion/recovery pulse sequence followed by cross-polarization. The proton spin-lattice relaxation times in the rotating frame ($T_{1\rho}^H$) were measured indirectly from observations of carbon atoms using a 90°–τ–spin lock pulse sequence prior to cross-polarization. Data acquisition was performed using ^{1}H decoupling, delay times (τ) ranging from 0.2 to 80 ms, and a contact time of 1.0 ms.

3. Results and discussion

3.1. Hydrogen bonding between PBZ and PCL

FTIR spectroscopy is a powerful tool for investigating specific intermolecular interactions. It has been reported that intermolecular hydrogen bonding plays a dominant role in determining the miscibility of polymers containing carbonyl or carbonate groups [26]. Fig. 1 presents infrared spectra of the PBZ/PCL 80/20 blend cured isothermally at 140, 160, and 180 °C for 30 min. There are two areas of interest in the infrared spectra of the blend: The hydroxyl group stretching region (from 3600 to 3200 cm^{-1}) and the carbonyl group stretching region (from 1780 to 1680 cm^{-1}). In Fig. 1(a), we observe that two components contribute to the spectra in the former region: One peak arises in the region 3540–3520 cm^{-1}, which we assign to free hydroxyl groups, and the other appears in the range 3420–3300 cm^{-1}, which we attribute to hydrogen-bonded hydroxyl groups. Upon curing at 140 °C for 30 min, a small absorbance appears that is due to the ring opening of the oxazine moiety in the benzoxazine. Further curing leads to increase in the intensity of the hydroxyl group stretching absorbance upon increasing the curing temperature. The non-hydrogen-bonding peaks remain almost in the same position (3532 cm^{-1}) upon curing, as should be expected for isolated hydroxyl groups. For the associated hydroxyl groups, the peak position shifted to lower frequencies as the curing process proceeded. Comparing the frequency difference ($\Delta\nu$) between the free and hydrogen-bonded hydroxyl groups allows the relative strength of this interaction to be evaluated. We observed that the value of $\Delta\nu$ was greater after higher-temperature curing than it was after curing at the lower temperature. Therefore, the hydrogen-bonding strength for the blend cured at 180 °C

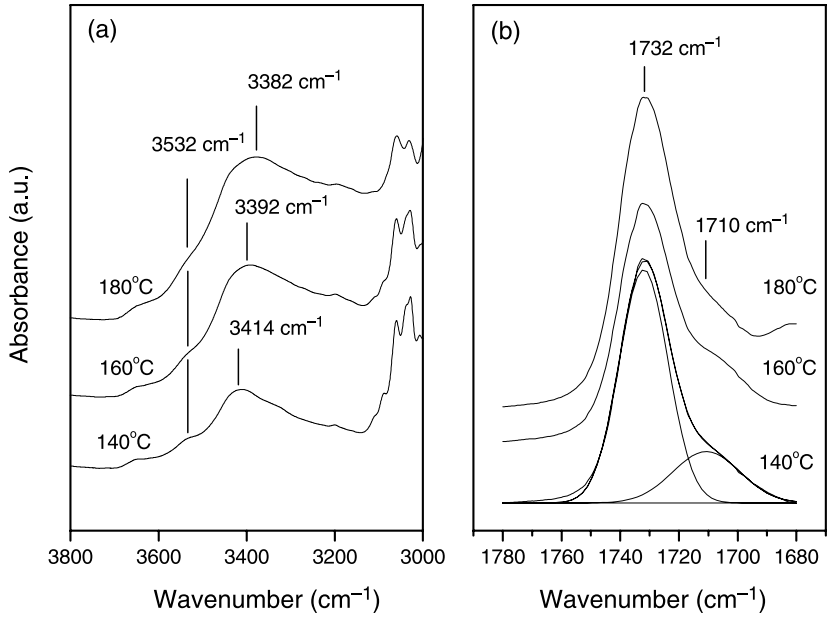

Fig. 1. FTIR spectra of the PBZ/PCL blend cured isothermally at 140, 160, and 180 °C for 30 min.

for 30 min ($\Delta\nu = 150\ cm^{-1}$) is relatively high when compared to that of the sample cured at 140 °C ($\Delta\nu = 118\ cm^{-1}$). In Fig. 1(b), we observe two bands in the region from 1780 to 1680 cm^{-1}: One band is centered at 1732 cm^{-1}, which we attribute to the characteristic peak of the non-hydrogen-bonded carbonyl groups, and the other is a relatively weak peak at 1710 cm^{-1}, which we assign to the hydrogen-bonded carbonyl groups. Upon curing, hydroxyl groups were produced—from the ring-opening reactions of the oxazine—which led to the formation of intermolecular hydrogen bonds with PCL. Therefore, the FTIR spectroscopy results demonstrate that hydrogen-bonding interactions do exist between the hydroxyl groups of the benzoxazine units and the carbonyl groups of PCL.

3.2. Thermal analyses

DSC analysis is one of the most convenient methods for determining the miscibility and thermal properties of polymer blends. A single composition-dependent glass transition is an indication of full miscibility on a dimensional scale between 10 and 30 nm [16,17]. Fig. 2(a) and (b) display DSC thermograms of pure PCL, pure PBZ, and their blends in the low- and high-temperature ranges, respectively. In blends having a PCL concentration $\geq$60 wt%, the resulting values of T_g are located within the range of PCL's T_g, whereas in the blends having a PCL content $\leq$40 wt%, the final values of T_g appeared within the PBZ range. We observed essentially only one value of T_g for all of the compositions. Fig. 3 depicts the relationship between the value of T_g of the blend and its PBZ content. The values of T_g for PCL and PBZ are −61 and 170 °C, respectively. Meanwhile, we observed for the blend a single value of T_g that is higher than that of either individual polymer. The large positive deviation indicates that strong interactions exist between the two polymers. The increase of T_g of the blend is due to the formation of a hydrogen bond network and the greater degree of polymerization, as has been reported previously by Ishida and Lee [27]. Fig. 4 displays DSC thermograms for PCL and its blends in the temperature range from 20 to 80 °C. The value of T_m of the PCL component decreased after blending with the amorphous PBZ. For the PCL component, T_m was 55.2 °C in the pure state and 52.1 °C in the 80/20 PBZ/PCL blend; i.e. the value of T_m decreased by ca. 3 °C (Fig. 4 and Table 1). This result indicates that the crystallization of PCL is affected by the presence of PBZ. In the blends, the crystallinity (X_c) of PCL can be calculated using the following equation:

$$X_c = \frac{\Delta H}{\Delta H^0 W} \quad (1)$$

where ΔH^0 is the melting enthalpy of 100% crystalline PCL (136 J/g) [28], ΔH is the apparent melting enthalpy

Table 1
Thermal properties of PBZ/PCL blends

Composition PBZ/PCL	T_m of PCL (°C)	ΔH^a (J/g)	X_c (%)	T_g (°C)
0/100	55.2	85.4	62.8	−60.3
20/80	54.2	76.9	56.5	−46.9
40/60	53.8	73.3	53.9	−41.3
60/40	52.9	62.6	46.0	206.4
80/20	52.1	51.0	37.5	189.6
100/0	–	–	–	170.3

[a] The enthalpy of melting is based on the weight fraction of PCL in the blend.

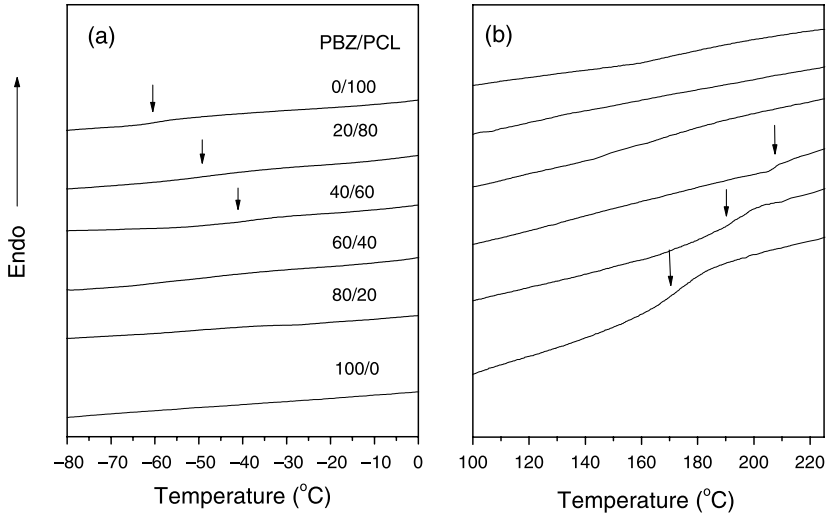

Fig. 2. DSC thermograms of PBZ, PCL, and their blends within the ranges (a) −80–0 °C and (b) 100–225 °C.

corresponding to the PCL component, and W is the weight fraction of PCL in the blend. Table 1 lists the calculated crystallinities. Obviously, the PCL component in the blends possessed a lower crystallinity than that in the pure state and its crystallinity decreased upon increasing the PBZ content. It has been demonstrated for blends having crystallizable components that the depression of both the crystallinity and the crystallization rate are indicative of the miscibility phenomena occurring in the amorphous state [29]. Similar behavior has been observed for PCL/PVPh blends; it was attributed to the increasing value of T_g [30]. For PBZ/PCL blends, this behavior should arise from the formation of the hydrogen bond network in addition to the increasing value of T_g. Accordingly, we conclude that PCL crystallization becomes more difficult when the morphology of the blend is dominated by PBZ.

3.3. Dynamic mechanical analysis

We performed dynamic mechanical analysis of the PBZ/PCL blends to observe the effect that PCL has on the thermomechanical properties of PBZ. Figs. 5 and 6 depict the dynamic mechanical spectra of pure PBZ, pure PCL, and their blends having PCL contents of 20 and 40 wt%. As Fig. 5 indicates, the maximum of the loss modulus (E'') corresponding to the glass transition temperature of PCL was −56 °C. The 60/40 PBZ/PCL blend displays two values of T_g: One at ca. −22 °C, which is higher than the value for pure PCL, and the other at ca. 184 °C, which is also higher than that of pristine PBZ. Owing to the presence of two glass transitions in the blend, this blend system is partially miscible. From a comparison of the storage modulus of PBZ and its blends, it is clear that the storage

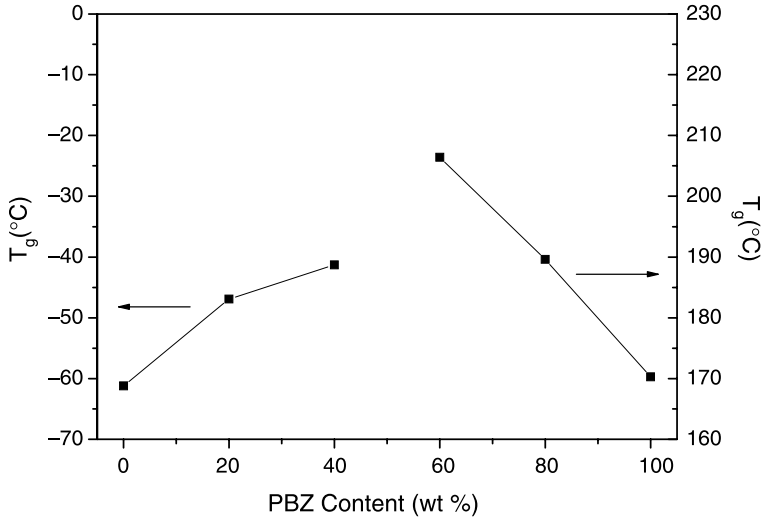

Fig. 3. The value of T_g plotted as a function of the PBZ content for cured PBZ/PCL blends.

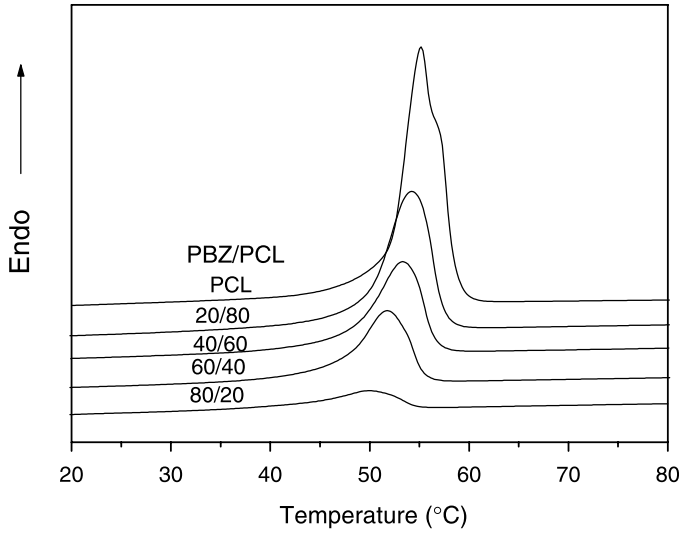

Fig. 4. DSC thermograms of PCL and PBZ/PCL blends recorded from the second heating scan.

modulus of the blend is lower than that of pure PBZ. From Fig. 5, we observe that, upon increasing the temperature, the logarithm of the storage modulus (log E') varies very little within the first section of the curve (the first plateau zone), but then a sharp decrease occurs, which we attribute to the change in the segmental mobility related to the glass transition. After a second plateau zone, the value of log E' again decreased dramatically because of melting of the crystalline phase; the melting temperature of the PCL was ca. 58 °C. The most pronounced effect of the presence of PCL was to broaden the glass transition region, judging from the peaks of E'' and the decrease of the storage modulus (E') in the transition region upon increasing the PCL content. The broadening of the E'' peak indicates an increase in the number of modes of branching, which results in a wider distribution of structures [31]. Fig. 6 reveals the loss tangents (tan δ) of pure PCL, pure PBZ, and their blends. We note three differences in the relaxation behavior of these samples. First, the α transition peak became broader upon increasing the PCL content. It may be reasonable to assume that there is an interfacial region, in addition to the amorphous region in pure PBZ, and that the size of this region increased after the addition of PCL because of the increasing sizes of the crystalline and amorphous regions. If so, this phenomenon would be one of the most significant reasons for the observed peak broadening. Second, the value of tan δ in the peak top decreased upon increasing the PCL content; this situation may be related to the phase structure and density of the hydrogen bond network. Third, the value of T_g, determined as the temperature corresponding to the maximum of tan δ in the α-transition, increased with the PCL content (Fig. 3). Because the glass transition process is

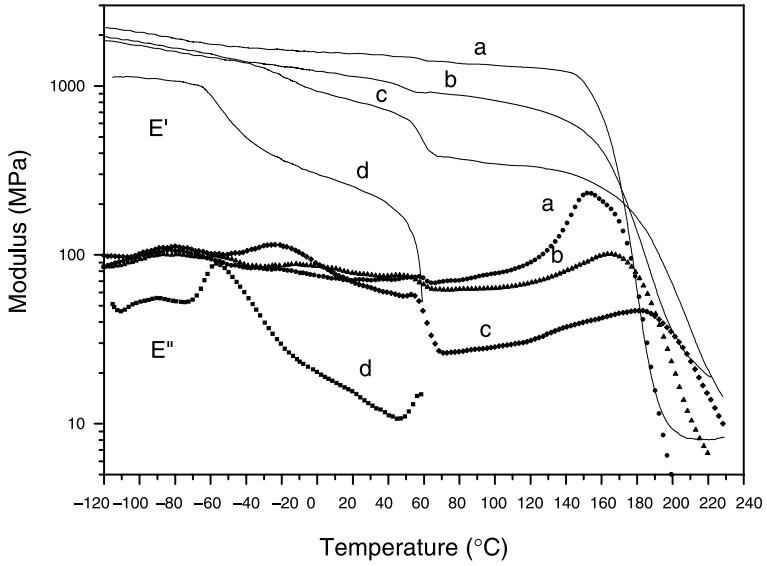

Fig. 5. Storage moduli (E') and loss moduli (E'') of PBZ/PCL blends having various PCL contents: (a) 0, (b) 20, (c) 40, (d) 100 wt%.

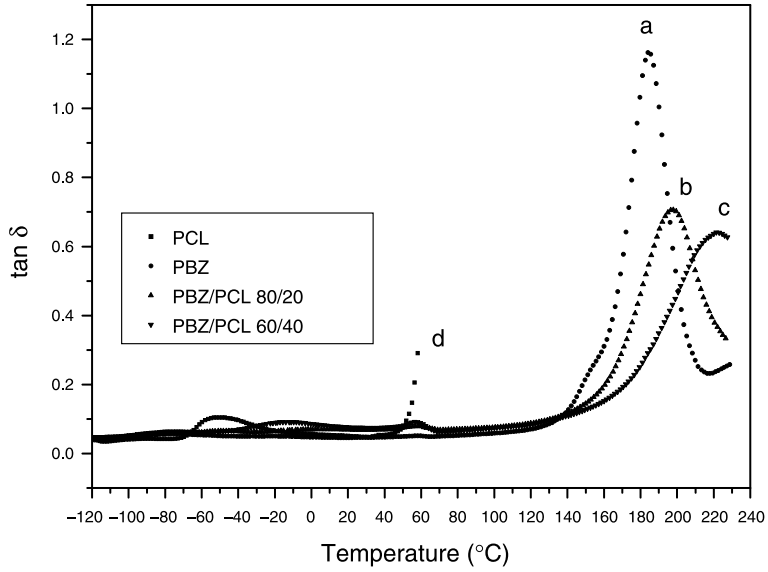

Fig. 6. Loss tangents (tan δ) of PBZ/PCL blends having various PCL contents: (a) 0, (b) 20, (c) 40, (d) 100 wt%.

related to molecular motion, the value of T_g is related to the molecular packing and the chain rigidity and linearity. The values of T_g of the PBZ/PCL blends increased as the PCL content increased, namely 185.4, 198.5, and 223.1 °C at PCL contents of 0, 20, and 40 wt%, respectively. This finding implies that the introduction of the PCL unit into PBZ can improve the properties of PBZ at high temperature. This result is in good agreement with those of the DSC measurements.

3.4. ^{13}C CP/MAS NMR spectra

Solid state ^{13}C NMR spectroscopy is a powerful tool for studying the structure and miscibility of polymer blends [18,19]. The chemical shifts and line shapes of ^{13}C nuclei in cross-polarization and magic-angle spinning (CP/MAS) spectra can identify the chemical environments of the carbon atoms in the blend, because the chemical shift and line shape are both highly sensitive to the local electron density. Fig. 7 displays ^{13}C CP/MAS NMR spectra recorded at room temperature for PBZ, PCL, and 60/40, 40/60, and 20/80 PBZ/PCL blends. The relatively broad resonance for PBZ and sharp resonance for PCL reflect the difference between their amorphous and semi-crystalline states, respectively. We observed five peaks for pure PCL. The signal at 174.8 ppm is attributable to the carbonyl (C=O) carbon atom. We note that the resonance appearing at 112.2 ppm is a side band of the resonance of the C=O carbon atom. The structure and peak assignments of PCL are provided below [32]:

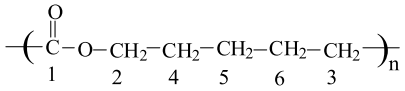

(PCL)

The pure PBZ displays six resonances: The one at 156.4 ppm corresponds to the hydroxyl-substituted carbon atom (C-1); all of the other assignments are given in Fig. 7 and are assigned below:

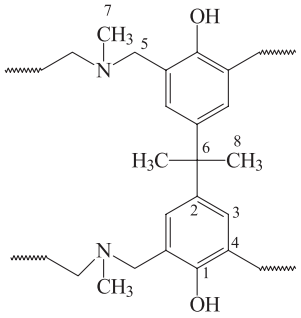

(PBZ)

The ^{13}C CP/MAS NMR spectra of B-a and B-m have been discussed in detail previously [24]. It is well know that specific interactions between polymer chains change the chemical environment of the neighboring molecules, which can cause changes in magnetic shielding and, hence, the chemical shift. In general, the ^{13}C nuclei exhibit downfield shifts when they are involved in hydrogen bonds. For PCL/novolac blends, the formation of a hydrogen bond between a carbonyl group in PCL and a hydroxyl group in novolac results in a downfield shift of ca. 2 ppm in the resonance of the C=O carbon atom [9]. In our case, however, we observed no detectable differences for the chemical shifts and line shapes of the pure components and their blends and, thus, we conclude that the chemical shifts of ^{13}C nuclei do not provide direct information regarding the interactions between PBZ and PCL.

3.5. Measurement of T_1^H

For polymer blends miscible on the molecular scale, the protons of different polymer chains can be closely coupled and relax at an identical rate through the spin-diffusion mechanism, whereas protons located far apart or in different environments relax at an independent rate. Therefore, the

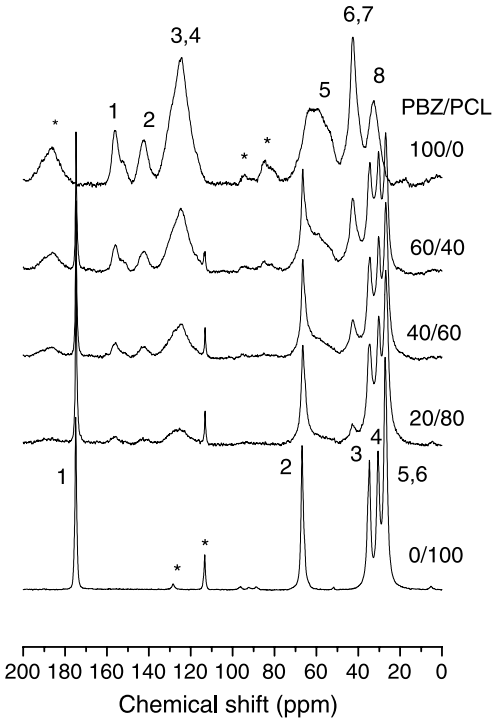

Fig. 7. ^{13}C CP/MAS NMR spectra of pure PBZ, PCL, and their blends. Asterisks denote spinning sidebands.

miscibility of a polymer blend can be investigated by determining the relaxation rates of protons corresponding to each polymer component. For such T_1^H experiments, we used the inversion recovery method and measured the resonance intensities of PBZ, PCL, and their blends as functions of delay time. According to the method used, the magnetization of a resonance's relaxation at a single exponential function should obey the following exponential equation:

$$M_\tau = M_\infty\left[1 - 2\exp\left(\frac{-\tau}{T_1^H}\right)\right] \tag{2}$$

where T_1^H is the proton spin-lattice relaxation time in the laboratory frame, τ is the relaxation time used in the experiment, M_τ is the corresponding resonance intensity, and M_∞ is the intensity of the resonance at $\tau \geq 5T_1^H$. After taking the natural logarithm of Eqs. (2) and (3) can be obtained:

$$\ln\left[\frac{M_\infty - M_\tau}{2M_\infty}\right] = \frac{-\tau}{T_1^H} \tag{3}$$

The value of T_1^H can be obtained from the slope of the plot of $\ln[(M_\infty - M_\tau)/(2M_\infty)]$ against τ. Fig. 8 displays logarithmic plots of the intensity of the resonance of the ^{13}C nuclei against the delay time for a selected carbon atom (at 174.8 ppm) of pure PCL and its blends. We observe that the experimental data fit quite well to the calculated values over the whole selected range of delay times, i.e. we obtained a straight line for each composition. The T_1^H relaxations at other sites also follow the single-exponential relaxation of Eq. (3). From the slopes of these plots, we obtained the values of T_1^H, which are summarized in Table 2 for PBZ, PCL, and their blends at different sites and at different compositions. The relaxation times T_1^H were 0.72 and 1.49 s for pure PBZ and PCL, respectively. From Table 2, we observe that the T_1^H values of the blends are intermediate between those of the pure polymers. In addition, the T_1^H values of all of the resonances of the carbon atoms for each blend are identical, as far as experimental error is concerned. These results indicate that spin diffusion among the protons within the T_1^H time scale is efficient enough to average out the intrinsic spin-lattice relaxation of the different domains. Thus, the domain sizes of these blends are smaller than the diffusion path length within the time T_1^H.

3.6. Proton spin-lattice relaxation ($T_{1\rho}^H$) analyses

The proton spin-lattice relaxation time in the rotating frame, $T_{1\rho}^H$, has been used widely to examine the heterogeneity of domains. A proton's $T_{1\rho}^H$, obtained via a resolved carbon atom's resonance, provides a convenient tool to access the complicated morphology of polymer blends and to characterize the molecular motion within polymers [20–22]. The values of $T_{1\rho}^H$ can be determined for protons within different morphological domains; the spin diffusion is weak and can be neglected if the coupled domain is large enough. In general, the intensity of magnetization displays a single exponential decay as a function of the spin-lock time. We calculated the values of $T_{1\rho}^H$ according to the exponential function model:

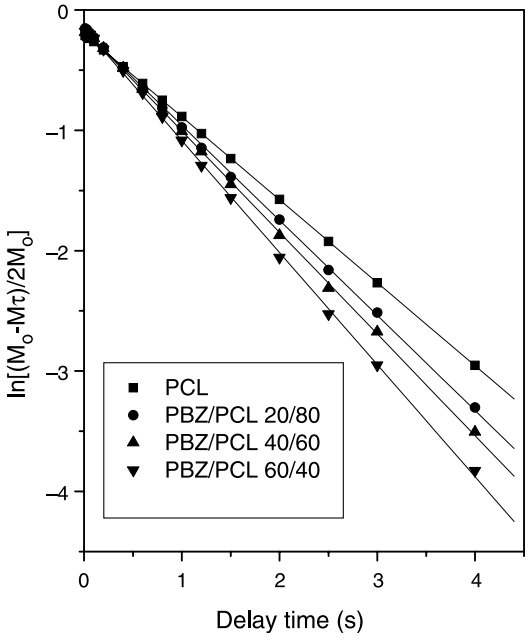

Fig. 8. Measuring T_1^H through logarithmic plots of resonance intensities (at 174.8 ppm) as a function of delay time: (a) PCL, (b) PBZ/PCL 20/80, (c) PBZ/PCL 40/60, (d) PBZ/PCL 60/40.

Table 2
Values of T_1^H for PBZ, PCL and their blends (units: s)

Composition PBZ/PCL	PCL 174. 8 ppm	PBZ 124. 3 ppm	PCL 66. 6 ppm	PBZ 42. 7 ppm
0/100	1.49		1.47	
20/80	1.26	–	1.24	–
40/60	1.08	1.03	1.05	1.01
60/40	0.96	0.92	0.94	0.91
100/0		0.72		0.72

The accuracy of the measurements is ±5%.

$$M(\tau) = M(0)\exp\left[\frac{-\tau}{T_{1\rho}^H}\right] \quad (4)$$

where $M(0)$ is the maximum magnetization; the values of $T_{1\rho}^H$ can be determined from the slopes in the plots of $\ln[M(\tau)/M(0)]$ against τ. Fig. 9 displays the magnetization decay curves of the C=O carbon atoms (174.8 ppm) as a function of the spin-lock times for PCL and its blends. We observe that the experimental data cannot be fitted to a straight line. In fact, a bi-exponential function must be used to simulate the relaxation process for these compositions. The normalized ^{1}H nuclei magnetization $[M(\tau)]$ of PCL is simulated by the bi-exponential function, which reflects the two relaxation rates of both domains as follows:

$$\frac{M(\tau)}{M(0)} = x_a\exp\left(\frac{-\tau}{T_{1\rho}^H, S}\right) + x_c\exp\left(\frac{-\tau}{T_{1\rho}^H, L}\right) \quad (5)$$

where $T_{1\rho}^H$, S and $T_{1\rho}^H$, L correspond to the relaxation times in the mobile and rigid components and x_a and x_c are the respective weight fractions of the domain. The values of $T_{1\rho}^H$ can be obtained from the slope of the plot of $\ln[M(\tau)/M(0)]$ versus the spin lock time; Table 3 summarizes the results. From Table 3, we observe two values of $T_{1\rho}^H$ for pure PCL, but only one for PBZ. This situation occurs because PCL is a semicrystalline polymer, whereas PBZ is an amorphous one. For a semicrystalline polymer, the proton spin-lattice relaxation rate in the crystalline phase will be different from that which occurs in the amorphous phase if the domain sizes of the crystalline and amorphous phases are larger than the spin-diffusion length within the relaxation time. In the case of PCL, the short component corresponds to the amorphous phase and the longer one (ca. 63 ms) to the crystalline phase [7]. In addition, it is evident that the PBZ carbon atoms exhibit another value of $T_{1\rho}^H$ that is different from those of PCL in the crystalline and amorphous phases. This result strongly suggests that PBZ and PCL are immiscible on the scale of the spin-diffusion path length within the $T_{1\rho}^H$ time for these blends.

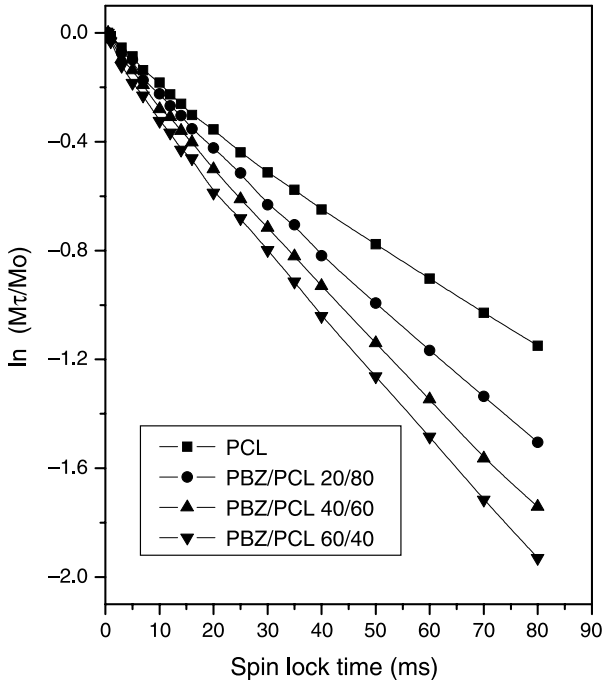

Fig. 9. Measuring $T_{1\rho}^H$ through logarithmic plots of resonance intensities (at 174.8 ppm) as a function of spin-lock time: (a) PCL, (b) PBZ/PCL 20/80, (c) PBZ/PCL 40/60, (d) PBZ.

It is well known that the molecular mobility of a polymer is affected by many factors, including its chemical structure, crystallinity, and degree of crosslinking. Fig. 10 displays the relationship between $T_{1\rho}^H$ and the crystallinity of PCL in the PBZ/PCL blends. In a previous study, we found that the value of $T_{1\rho}^H$ correlated linearly with the crystallinity rather well for poly(ethylene terephthalate) [33]. As expected, $T_{1\rho}^H$ increases upon increasing PCL crystallinity, as can be observed in Fig. 10, which displays a linear relationship between $T_{1\rho}^H$ and X_c within experimental error. Furthermore, from Table 3, the decrease in the value of $T_{1\rho}^H$ of the PCL can be used directly to measure the increase in PCL's molecular mobility upon increasing the PBZ content. This observation suggests that the crystallinity of PCL is one of the main factors affecting the molecular mobility of PCL.

3.7. Determining domain size

From DSC measurements, we observed that all compositions of PBZ/PCL blends were homogeneous because they displayed a single value of T_g, but this situation does not necessarily imply homogeneity of the blend on the nanometer scale. To explore the miscibility of the blends further, T_1^H and $T_{1\rho}^H$ relaxation experiments can provide an estimate of the diffusive path length and, hence, the sizes of

Table 3
Values of $T_{1\rho}^H$ for PBZ, PCL, and their blends (units: ms)

PBZ/PCL	PCL 174. 8 ppm	PBZ 124. 3 ppm	PCL 66. 6 ppm	PBZ 42. 7 ppm
0/100	13.1/63.1		12.9/61.0	
20/80	10.1/52.8	–	9.8/51.2	–
40/60	8.2/49.2	7.3	8.1/48.0	7.0
60/40	6.4/45.5	8.6	5.9/44.1	8.5
100/0		11.4		11.1

The accuracy of the measurements is ±5%.

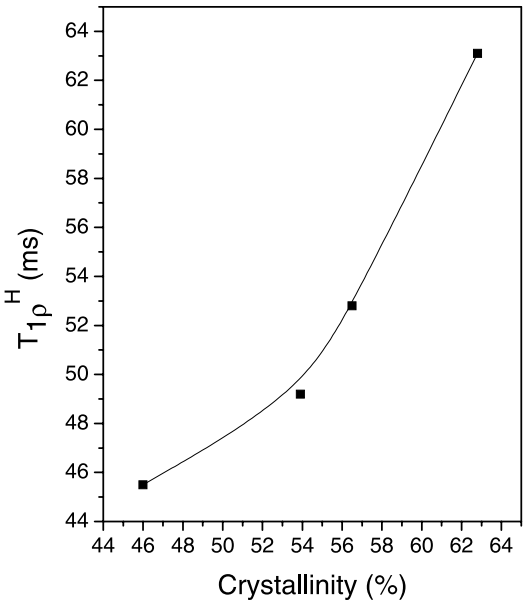

Fig. 10. Values of $T_{1\rho}^{H}$ (174.8 ppm) plotted as a function of PCL crystallinity in PBZ/PCL blends.

a blend's heterogeneities. If the diffusion length is smaller than the dimensions of the domains in the blends, protons in each component will decay independently of one another and a double exponential decay will be observed. In contrast, if the diffusion length is much larger than the dimensions of the domains in the blend, spin diffusion occurs between both components. A useful approximation of the upper limit to the domain size can be estimated using the equation [34–36]

$$\langle L \rangle = (6DT_i)^{1/2} \tag{6}$$

where $\langle L \rangle$ is the average diffusive path length for the effective spin diffusion and D is the spin-diffusion coefficient, which depends on both the average proton-to-proton distance and the strength of the dipolar interaction; it has a typical value of $4\text{–}6\times10^{-16}\,\mathrm{m^2\,s^{-1}}$. For the $T_{1\rho}^{H}$ experiment, D is half of this value. The term T_i is the relaxation time, namely T_1^H or $T_{1\rho}^H$, according to the type of relaxation measurement. From the measured values of T_1^H (from Table 2) and Eq. (6), we estimate that the PBZ/PCL blends are intimately mixed on a scale below 40–70 nm. As in the $T_{1\rho}^{H}$ experiment, the values of $T_{1\rho}^{H}$ obtained from PBZ are different from that of PCL for all compositions, which implies that the domain sizes of the blends are larger than the effective diffusion path length within the $T_{1\rho}^{H}$ time scale. Using observed $T_{1\rho}^{H}$ relaxation times (from Table 3) and the spin-diffusion coefficient D, we observe that PBZ and PCL are not miscible on a scale of 2–4 nm. From these results, we conclude that the domain sizes between PCL and PBZ are smaller than the T_1^H measurement scale (40–70 nm), but larger than the $T_{1\rho}^{H}$ measurement scale (2–4 nm).

4. Conclusions

In this study, we prepared PBZ/PCL blends by solution blending of benzoxazine monomer and PCL, followed by the thermal curing of benzoxazine. The addition of PCL to the PBZ network greatly increases the crosslink densities and strongly influences its thermal properties. FTIR spectroscopy measurements indicated that hydrogen bonding exists between the carbonyl groups of PCL and the hydroxyl groups of PBZ upon curing. DSC results indicated that both the melting temperature and degree of crystallinity of the PCL component in the blend decreased upon increasing the PBZ content. We observed a single glass transition temperature for each blend; its value increased upon increasing the content of PCL. Two glass transitions appeared, however, in the blends having higher PCL concentrations; this finding suggests that this blend system is only partially miscible. ^{13}C CP/MAS NMR spectroscopic analyses revealed that the values of T_1^H of the blends were intermediate between those of the pure polymers. Furthermore, we obtained single T_1^H decays for all of the blends and the values of T_1^H of all of the carbon atoms' resonances remained the same within experimental error. These results indicate that spin diffusion among the protons within the T_1^H time scale is efficient enough to average out the intrinsic spin-lattice relaxation of the different domains. We observed, however, a bi-exponential decay of the PCL component in the $T_{1\rho}^H$ experiments, which indicates the presence of crystalline and amorphous phases in the blends. In addition, the PBZ carbon atoms exhibit another $T_{1\rho}^H$ value that is different from that of PCL in either the crystalline or amorphous phase. This result strongly suggests that PBZ and PCL are immiscible on the scale of the spin-diffusion path length within the $T_{1\rho}^H$ time for these blends. From our T_1^H and $T_{1\rho}^H$ results, we conclude that PBZ/PCL blends are homogeneous on the scale of 40–70 nm, but are heterogeneous on the scale of 2–4 nm.

Acknowledgements

We thank the National Science Council, Taiwan, Republic of China (NSC-91-2216-E-238-001), and Vanung University for financial support.

References

[1] Ning X, Ishida H. J Polym Sci, Polym Chem Ed 1994;32:1121.
[2] Ning X, Ishida H. J Polym Sci, Polym Phys Ed 1994;32:921.
[3] Ishida H, Low H. Macromolecules 1997;33:1099.
[4] Shyan BS, Ishida H. Polym Compos 1996;17:710.
[5] Agag T, Takeichi T. Macromolecules 2003;36:6010.
[6] Su YC, Chang FC. Polymer 2003;44:7989.
[7] Wang J, Cheung MK, Mi Y. Polymer 2002;43:1357.
[8] Mandal TK, Woo EM. Polym J 1999;31:226.
[9] Zhong Z, Guo Q, Mi Y. Polymer 1999;40:27.

[10] Ishida H, Lee YH. Polymer 2001;42:6971.
[11] Zheng S, Lu H, Guo Q. Macromol Chem Phys 2004;205:1547.
[12] Zhang SH, Jin X, Painter PC, Runt J. Macromolecules 2003;36:5710.
[13] Huang JM. J Polym Sci, Polym Phys Ed 2004;42:1694.
[14] Kuo SW, Huang CF, Wu CH, Chang FC. Polymer 2004;45:6613.
[15] He Y, Asakawa N, Inoue Y. J Polym Sci, Polym Phys Ed 2000;38: 1848.
[16] Utracki LA. Polymer alloy and blends. Munich, Germany: Hanser Publishers; 1989.
[17] Kaplan DS. J Appl Polym Sci 1976;20:2615.
[18] Mathias LJ. Solid state NMR of polymers. New York: Plenum Press; 1988.
[19] Ibbett RN. NMR spectroscopy of polymers. London: Blackie Academic and Professional; 1993.
[20] Stejskal EO, Schaefer J, Sefcik MD, Mckay RA. Macromolecules 1981;14:275.
[21] Wang J, Cheung MK, Mi Y. Polymer 2001;42:2077.
[22] Hill DJT, Whittaker AK, Wong KW. Macromolecules 1999;32:5285.
[23] Russell VM, Koenig JL, Low HY, Ishida H. J Appl Polym Sci 1998; 70:1401.
[24] Russell VM, Koenig JL, Low HY, Ishida H. J Appl Polym Sci 1998; 70:1413.
[25] Goward GR, Sebastiani D, Schnell I, Spiess HW, Kim HD, Ishida H. J Am Chem Soc 2003;125:5792.
[26] Kuo SW, Huang CF, Chang FC. J Polym Sci, Polym Phys Ed 2001;39: 1348.
[27] Ishida H, Lee YH. J Polym Sci, Polym Phys Ed 1994;32:921.
[28] Kwei TK. J Polym Sci, Polym Phys Ed 1984;22:307.
[29] Rong M, Zeng H. Polymer 1997;38:269.
[30] Lezcano EG, Salon CC, Prologo MG. Polymer 1996;37:3603.
[31] Agag T, Takeichi T. Polymer 1999;40:6557.
[32] Newmark RA, Runge ML, Chermark JF. J Polym Sci, Polym Chem Ed 1981;19:1329.
[33] Huang JM, Chu PP, Chang FC. Polymer 2000;41:1741.
[34] McBrierty VJ, Packer J. Nuclear magnetic resonance in solid polymers. Cambridge: Cambridge University Press; 1993.
[35] Demco DE, Johannsson A, Tegenfeldt J. Solid State Nucl Magn Reson 1995;4:13.
[36] Clauss J, Schmidr-Rohr K, Spiess HW. Acta Polym 1993;44:1.